Title

Intramolecular sensitization of americium luminescence in solution: shining light on short-lived forbidden 5f transitions

Journal

Dalton Transactions, 45(24)

ISSN

1477-9226

Authors

Sturzbecher-Hoehne, M
Yang, P
D'Aléo, A
et al.

Publication Date

2016-06-14

DOI

10.1039/c6dt00328a

Peer reviewed

Dalton Transactions

PAPER

View Article Online
View Journal | View Issue

Cite this: *Dalton Trans.*, 2016, **45**, 9912

Intramolecular sensitization of americium luminescence in solution: shining light on short-lived forbidden 5f transitions†

M. Sturzbecher-Hoehne,[a] P. Yang,*[b] A. D'Aléo*[c] and R. J. Abergel*[a]

Received 22nd January 2016,
Accepted 25th February 2016

DOI: 10.1039/c6dt00328a

www.rsc.org/dalton

The photophysical properties and solution thermodynamics of water soluble trivalent americium (Am^{III}) complexes formed with multidentate chromophore-bearing ligands, 3,4,3-LI(1,2-HOPO), Enterobactin, and 5-LIO(Me-3,2-HOPO), were investigated. The three chelators were shown to act as antenna chromophores for Am^{III}, generating sensitized luminescence emission from the metal upon complexation, with very short lifetimes ranging from 33 to 42 ns and low luminescence quantum yields (10^{-3} to 10^{-2}%), characteristic of Near Infra-Red emitters in similar systems. The specific emission peak of Am^{III} assigned to the $^5D_1 \rightarrow {}^7F_1$ f–f transition was exploited to characterize the high proton-independent stability of the complex formed with the most efficient sensitizer 3,4,3-LI(1,2-HOPO), with a $\log \beta_{110} = 20.4 \pm 0.2$ value. In addition, the optical and solution thermodynamic features of these Am^{III} complexes, combined with density functional theory calculations, were used to probe the influence of electronic structure on coordination properties across the f-element series and to gain insight into ligand field effects.

Introduction

The past several years have seen an increased resurgence of interest in nuclear power from many countries, with the common goals of ensuring sustainable energy supplies and curbing greenhouse gases.[1,2] However, while proceeding at a rapid rate, the development of nuclear energy is still hampered by safety concerns associated with the handling and processing of spent nuclear fuel and high-level nuclear waste.[3,4] The long-term radioactivity of nuclear waste repositories is one of the main issues at stake, and is in part determined by the presence of minor trivalent actinides such as americium (Am^{III}) and curium (Cm^{III}).[5–7] The separation of these metal ions from each other and from trivalent lanthanides has proven inherently difficult due to their similar chemical properties and remains a great technical challenge for advanced transmutation and irradiated fuel-reprocessing operations.[8] Approaches for separation range from established solvent extraction techniques such as the TALSPEAK process that relies on selective complexing agents and cation exchanging extractants[9,10] to more recent methods that combine oxidation and ion exchange procedures.[11] The complexity of these approaches and the further need for effective separation processes direly call for a better understanding of the fundamental coordination chemistry of trivalent actinides as well as for precise methods to detect, characterize, and differentiate these metal ions in solution.

Several lanthanides and actinides, including Am^{III} and Cm^{III}, are known to display specific luminescence properties,[12–15] which can provide important information on the electronic and chemical differences between the 4f and 5f elements and may be in turn used for speciation determination. Most prior actinide photo-luminescence studies have been performed in the solid state and are based on direct excitation of the metal centered transitions, which necessitates high excitation power in order to populate emissive states and generate weak luminescence signals attributed to Laporte-forbidden f–f transitions.[16–22] In contrast, most of our recent work has focused on the indirect modulation of actinide luminescence through the use of sensitizing antenna chelators.[23–25] In this process, luminescence of the metal ion is prompted by the excitation of the ligand and subsequent intramolecular energy transfer from a triplet excited state or a singlet intra-ligand charge-transfer excited state of the ligand to the metal ion.[12,26] Using the so-called "antenna" effect therefore leverages the much larger molar absorption coefficients of organic chromophores as compared to those of the weakly absorbing f–f transitions of actinide and lanthanide ions.

Siderophore-inspired hydroxypyridinone (HOPO)-containing multidentate ligands are flagship chelators currently under

[a]*Chemical Sciences Division, Lawrence Berkeley National Laboratory, Berkeley, CA 94720, USA. E-mail: rjabergel@lbl.gov; Fax: +1 510 486 5596; Tel: +1 510 486 5249*
[b]*Theoretical Division, Los Alamos National Laboratory, Los Alamos, NM 87545, USA. E-mail: pyang@lanl.gov*
[c]*Aix Marseille Université, CNRS, CINaM UMR 7325, 13288 Marseille, France. E-mail: daleo@cinam.univ-mrs.fr*

†Electronic supplementary information (ESI) available. See DOI: 10.1039/C6DT00328A

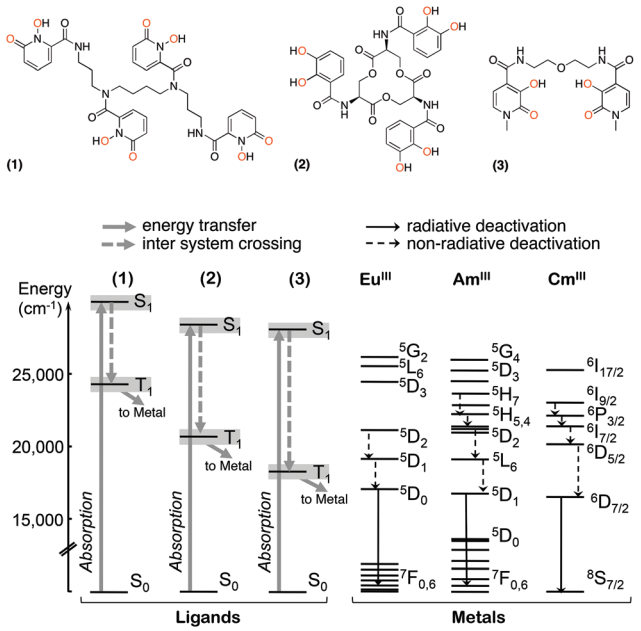

Fig. 1 Top: structures of 3,4,3-LI(1,2-HOPO) (**1**, left), Enterobactin (**2**, centre), and 5-LIO(Me-3,2-HOPO) (**3**, right). Bottom: simplified Jablonski diagram depicting the sensitization of Eu^{III}, Am^{III}, and Cm^{III} by the ligands **1**, **2**, and **3**.

scrutinized development as therapeutic actinide decontamination agents.[27] They are also known for their propensity to act as luminescence antenna for Cm^{III} and a variety of trivalent lanthanides,[25,28] and, based on the relative electronic energy levels of metals from the 4f and 5f series,[13,29] should therefore also act as antenna chromophores for Am^{III} (Fig. 1). The $5f^6$ configuration of Am^{III} makes it isoelectronic with Eu^{III} ($4f^6$), only differing from the lanthanide ion over its larger spin–orbit coupling and crystal field splitting, a smaller value of the Slater parameter, and a slightly larger ionic radius induced by the presence of 5f electrons.[30] Thus, Am^{III} displays the same ground- and excited-states symbol terms as Eu^{III} but with different energies,[29] which results in $^5D_1$ (17 200 cm^{-1}) being the emissive state in Am^{III}, whereas Eu^{III} emission arises from the higher energy state $^5D_0$ (17 500 cm^{-1}) and $^5D_1$ is the best accepting state in Eu^{III}.[31] In the work presented here, the sensitization of Am^{III} luminescence was attempted and characterized using three different ligand structures that display different triplet excited state energies above that of the Am^{III} $^5D_1$ state. Expanding on early observations by Yusov,[32] we report the first thorough characterizations and quantifications of the antenna effect in Am^{III}, using (i) the octadentate synthetic chelator 3,4,3-LI(1,2-HOPO) (**1**, Fig. 1) that bears four 1-hydroxy-pyridin-2-one (1,2-HOPO) moieties on a spermine scaffold, (ii) the natural hexadentate siderophore Enterobactin (**2**, Fig. 1) that links three catecholamide metal-binding groups to a cyclic tri-serine lactone, and (iii) the tetradentate synthetic ligand 5-LIO(Me-3,2-HOPO) (**3**, Fig. 1) that connects two *N*-methyl-3-hydroxy-pyridin-2-one (Me-3,2-HOPO) subunits onto a linear ether backbone through amide linkages. The Am^{III} complexes formed with these three compounds exhibit sharp luminescence features that were used to probe and discuss coordination chemistry properties as compared with corresponding lanthanide and Cm^{III} complexes, evidencing new tools for the speciation and characterization of minor trivalent actinide species.

Experimental

Caution: ^{243}Am and ^{248}Cm are hazardous radionuclides with high specific activities that should only be manipulated in specifically designated facilities, in accordance with appropriate safety controls.

General considerations

Chemicals were acquired from commercial suppliers and were used as received. Enterobactin was obtained from Prof. K. N. Raymond (Department of Chemistry, University of California at Berkeley). The ligands 3,4,3-LI(1,2-HOPO) and 5-LIO(Me-3,2-HOPO) were prepared and characterized as previously described.[33] The $LnCl_3{\cdot}nH_2O$ lanthanide salts utilized were of the highest purity available (>99.9%). Aliquots of acidified stocks of carrier-free ^{243}Am and ^{248}Cm (95.78% ^{248}Cm, 4.12% ^{246}Cm, 0.06% ^{245}Cm, 0.02% $^{244}Cm/^{247}Cm$ isotopic distribution by atom percentage) from the Lawrence Berkeley National Laboratory were used in this work. All solutions were prepared using deionized water purified by a Millipore Milli-Q reverse osmosis cartridge system and the pH was adjusted as needed with concentrated HCl or KOH. The pH of solutions was measured with a conventional pH meter at 25 °C (Metrohm Brinkmann) that was equipped with a glass electrode (Micro Combi, Metrohm) filled with KCl and calibrated with pH standards. Stock solutions of ligands were prepared in Milli-Q water further degassed by boiling for 1 h while being purged under Ar. Metal stock solutions were prepared in 0.1 mol L^{-1} HCl previously standardized by titrating against TRIS. For direct spectroscopic measurements, equimolar amounts of metal and chelator were used to constitute complex solutions (3 μmol L^{-1}, pH 7.4) in 0.1 mol L^{-1} HEPES buffer.

Photophysics

UV-Visible absorption spectra were recorded either on a Varian Cary 6000i double beam absorption spectrometer, NanoDrop 2000C, or Ocean Optics USB 4000, using quartz cells of 1.00 cm path length. Emission spectra were acquired on a HORIBA Jobin Yvon IBH FluoroLog-3 spectrofluorimeter, used in steady state mode. Spectra were reference corrected for both the excitation light source variation (lamp and grating) and the emission spectral response (detector and grating). Luminescence lifetimes were determined on a HORIBA Jobin Yvon IBH FluoroLog-3 spectrofluorimeter, adapted for time-correlated single photon counting (TCSPC) and multichannel scaling (MCS) measurements. To measure lifetimes >15 μs, a sub-microsecond Xenon flashlamp (Jobin Yvon, 5000XeF) was used as the lightsource, with an input pulse energy (100 nF

discharge capacitance) of *ca.* 50 mJ, yielding an optical pulse duration of less than 300 ns at full width at half maximum (FWHM). For shorter lifetimes, samples were excited with a pulsed NanoLED source (Jobin Yvon, N-16, pulse duration 1.1 ns; maximum repetition rate 1.0 MHz; peak excitation 330 nm). Spectral selection was achieved by passage through a double grating excitation monochromator (2.1 nm mm^{-1} dispersion, 1200 grooves per mm). Emission was monitored perpendicular to the excitation pulse, again with spectral selection. A thermoelectrically cooled single photon detection module (HORIBA Jobin Yvon IBH, TBX-04-D) incorporating fast rise time photo-multiplier tubes (PMT), wide bandwidth preamplifier, and picosecond constant fraction discriminator, was used as the detector. Signals were acquired using an IBH DataStation Hub photon counting module and data analysis was performed using the commercially available DAS 6 decay analysis software package from HORIBA Jobin Yvon IBH. Goodness of fit was assessed by minimizing the reduced chi squared function, and visual inspection of the weighted residuals. Each trace contained at least 5000 points, and the estimated error on the reported lifetime values is ±10%. Quantum yields were determined as previously described[25] and detailed in the ESI.† The q values were calculated by using eqn (1)[34] and (2)[35] for Cm^{III} and Am^{III} species, respectively.

$$q = 0.65\ k_{obs} - 0.88 \quad (1)$$

$$q = 2.56 \times 10^{-7}\ k_{obs} - 1.43 \quad (2)$$

Solution thermodynamics

General considerations. A Micro Combi (Metrohm) glass electrode (response to [H+] calibrated before each titration) was used with a Metrohm Titrando 907 (Metrohm) to measure the pH of the experimental solutions. All thermodynamic measurements were conducted at 25 °C, in 0.1 mol L^{-1} KCl supporting electrolyte under positive Ar gas pressure.

Spectrofluorimetric competition batch titrations. Varying volumes of a Eu^{III} (or Am^{III}, respectively) stock solution were added to solutions of ligand and Am^{III} (or Eu^{III}, respectively) in 0.1 mol L^{-1} KCl buffered at pH 7.4 with 0.1 mol L^{-1} HEPES. All solutions were diluted to identical volumes to reach final concentrations of ligand and Am^{III} (or Eu^{III}, respectively) of 3 μmol L^{-1}, and the ratio $[Eu^{III}]:[Am^{III}]$ (or $[Am^{III}]:[Eu^{III}]$, respectively) was comprised between 0 and 7 (or 0 and 5, respectively). Samples were equilibrated in a thermostatic shaker at 25 °C for two hours. The emission spectrum of each solution was measured using a 1 cm quartz cell (λ_{exc} = 325 nm, λ_{em1} = 595–620 nm, λ_{em2} = 695–710 nm). Each titration was performed independently twice and included over 20 data points. The data were then imported into the refinement program HypSpec[36,37] and analysed by nonlinear least-squares refinement.

Data treatment. All equilibrium constants were defined as cumulative formation constants, β_{mlh} according to eqn (3), where the metal and ligand are designated as M and L, respectively.

$$mM + lL + hH \rightleftharpoons [M_mL_lH_h]; \beta_{mlh} = \frac{[M_mL_lH_h]}{[M]^m[L]^l[H]^h} \quad (3)$$

All metal and ligand concentrations were held at estimated values determined from the volume of standardized stock solutions. The refinements of the overall formation constant β_{110} included the four previously determined ligand protonation constants,[38] the metal hydrolysis products for both competing metals, for which equilibrium constants were fixed to the literature values,[39] and the previously determined β_{110} and β_{111} Eu^{III} complex constants;[28] all ligand species formed with Am^{III} or Eu^{III} were considered to have significant emission to be observed in the emission spectra. The pM(Am^{III})‡ value was calculated using the modelling program Hyss.[40,41]

Density functional theory calculations

First principle calculations were performed using PBE exchange–correlation functional[42] implemented in the Amsterdam Density Functional (ADF 2014.07) program.[43–45] Scalar relativistic effects were taken into account by the ZORA formalism to the Dirac equation.[46] TZ2P basis sets with small cores were used for geometry optimization and QZ4P were used for property analysis.[47] Initial coordinates used for geometry optimization were obtained from published X-ray diffraction studies.[48]

Results and discussion

Sensitization of Am^{III} complexes

As introduced earlier (*vide supra*), the use of antenna ligands is known to result in the sensitization of, and brighter emission from, selected trivalent lanthanide or actinide ions,[26] making spectro-fluorimetric measurements possible even at very low concentrations with, in this case, minimum amounts of radioactive metal. The photophysical properties of the Am^{III} complexes formed *in situ* with **1**, **2**, and **3** were investigated in buffered aqueous solutions at pH 7.4 with 1 : 1 metal : ligand stoichiometries and concentrations of Am^{III} of the order of 3 μmol L^{-1}; the relevant parameters are summarized in Table 1. As expected the maxima of the electronic UV-visible absorption of the Am^{III} complexes, due to $\pi \rightarrow \pi^*$ transitions, are located in the UV part of the spectrum, spanning from 315 to 345 nm (Fig. 2 and Table 1), at the same energies as those observed for the corresponding lanthanide and Cm^{III} complexes (previously published results[25,28] in the case of **1** and **3** and new data on Eu^{III} and Cm^{III} complexes of **2**, ESI Fig. S1 and Table S1†).

The occurrence and efficiency of the antenna intramolecular energy transfer process in emitting metal complexes will greatly depend on the energy of the sensitizing ligand triplet excited state, which may be estimated by measuring the residual phosphorescence emission of the ligand singlet and

‡ The conditional stability constant pM is the −log [free M] for the specific set of conditions [metal] = 10^{-6} M, [ligand] = 10^{-5} M, pH 7.4.

Table 1 Photophysical parameters for Am^{III} complexes formed with ligands **1**, **2**, and **3** [a]

	1	**2**	**3**
λ_{max} (nm)	316	340	342
ε_{max} (mol^{-1} L cm^{-1})	17 750	13 320	23 940
λ_{exc} (nm)	325	345	345
Φ_{tot} (H_2O)[b]	1.0×10^{-4}	6.2×10^{-5}	1.3×10^{-5}
τ_{obs} (ns)[b]	42 (56[c], 73[d])	37	33

[a] All values reported are the results of at least three independent experiments performed in aqueous buffered solutions (0.1 mol L^{-1} HEPES, pH 7.4). [b] Uncertainties determined from the standard deviation between three independent measurements are within 10% of the given value. [c] In 25 : 75 (v : v) D_2O : H_2O. [d] In 50 : 50 (v : v) D_2O : H_2O.

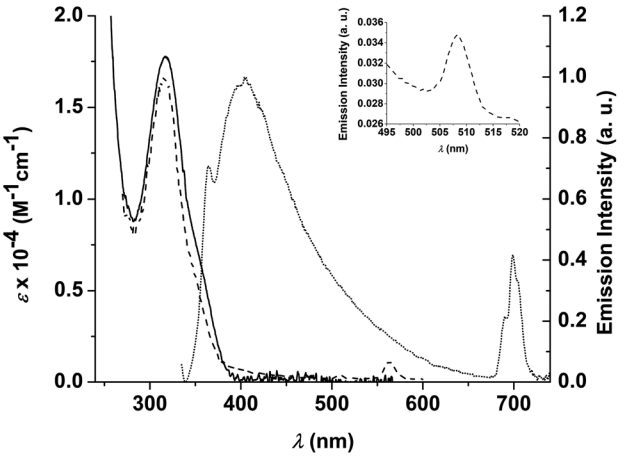

Fig. 2 Electronic absorption (solid, left) and normalized steady-state emission (solid, right, λ_{exc} = 325 nm) and excitation spectra (dashed, λ_{em} = 700 nm) of $[Am^{III}(\mathbf{1})]^-$, in 0.1 mol L^{-1} HEPES buffer (pH 7.4). **Inset**. Magnification of $[Am^{III}(\mathbf{1})]^-$ excitation spectra (λ_{em} = 700 nm), revealing an absorption band due to the Am^{III} $^5L_6 \leftarrow {}^7F_0$ transition.

triplet excited states in the corresponding Gd^{III} complexes, as described elsewhere and detailed in the ESI.†[38] The lowest triplet excited state of **1** had previously been determined by this technique at 24 390 cm^{-1},[38] an adequate level for the sensitization of most lanthanide ions as well as Cm^{III}.[25,28] That energy level is typical of the 1,2-HOPO chromophore and was found higher than those of the CAM- and Me-3,2-HOPO-based ligands, **2** and **3**, which were respectively determined at 20 600 and 18 650 cm^{-1}. Hence all three ligands were predicted to efficiently populate the $^5D_1$ emitting level of Am^{III} (Fig. 1). Upon excitation of $[Am^{III}(\mathbf{1})]^-$ at 325 nm, in the 1,2-HOPO $\pi \rightarrow \pi^*$ transition, two distinct emissions were observed: a broad band, centered at 405 nm, attributed to the residual singlet excited state emission from the chelating moieties (with a fluorescence quantum yield of 0.13%), and a much less intense structured emission pattern centered at 700 nm that was ascribed to the Am^{III} $^5D_1 \rightarrow {}^7F_1$ transition (Fig. 2). It is also clear from the excitation spectrum collected at 700 nm (Fig. 2) that the Am^{III} emission arises from the $\pi \rightarrow \pi^*$ transitions of the 1,2-HOPO ligand, a direct evidence of the antenna effect.

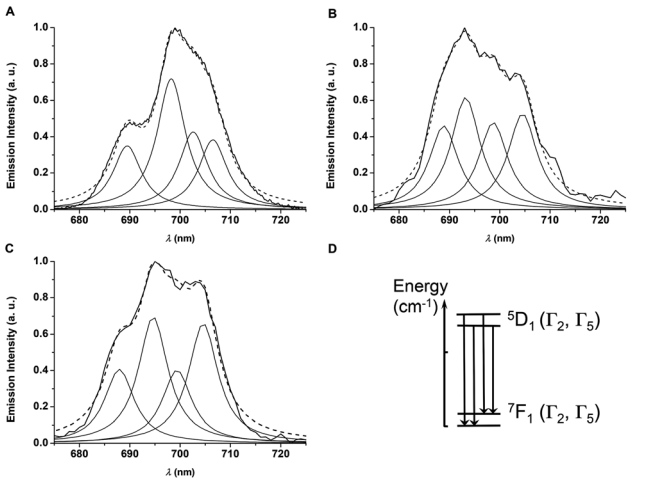

Fig. 3 Deconvolution of the normalized Am^{III} emission peak for ligands **1** (A), **2** (B), and **3** (C); solid and dashed lines represent the original spectra and fits, respectively. (D) Simplified depiction of the Stark levels of the emitting $^5D_1$ and accepting $^7F_1$ states.

Finally, attempts to directly excite this forbidden f–f transition under the same conditions resulted in no emission, a consequence of its low molar absorption coefficient, as compared with the highly accessible singlet $\pi \rightarrow \pi^*$ transition of the 1,2-HOPO units (*i.e.* ε values of 100 mol^{-1} L cm^{-1} *vs.* 17 750 mol^{-1} L cm^{-1}). Together, these data perfectly illustrate the advantage of using an antenna chromophore to increase complex brightness§ by exciting the ligand rather than directly exciting the f–f transitions (*i.e.* brigthness values of 1.8 mol^{-1} L cm^{-1} *vs.* 0.01 mol^{-1} L cm^{-1}).

Similarly, Am^{III} emission was observed upon ligand excitation in the complexes formed with **2** and **3**, allowing us to assert that the triplet excited states of the sensitizing chromophores (*i.e.* 1,2-HOPO, CAM, and Me-3,2-HOPO) within this series of chelates lie at adequate energies relative to the Am^{III} $^5D_1$ level. As evidenced in Fig. 3, the structure of the characteristic Am^{III} emission varies with the coordinating ligand, a result from ligand field splitting of the metal emitting and accepting states. Deconvolution of this emission band using Lorentzian functions revealed the participation of four transitions between different J = 1 Starks levels: two $^5D_1$ (Γ_2, Γ_5) emitting and two $^7F_1$ (Γ_2, Γ_5) accepting levels. For all three complexes, the most intense contribution (from 29 to 39%, centered between 693.2 and 698.3 nm) is assigned as originating from the lowest Stark level of the $^5D_1$ state to the lowest one of the $^7F_1$ state (ESI Table S2†). However, the relative contributions of the different states are more equally distributed for **2** and **3**, indicative of a higher symmetry for the complexes formed with those two ligands and geometry distortions different from that of the $[Am^{III}(\mathbf{1})]^-$ complex.

§ The brightness is defined as the product of molar absorption coefficient and luminescence quantum yield, and it represents the capacity of the complex to absorb photons multiplied by its capacity to emit photons.

Efficiency of the antenna process

Upon further measurement accumulations focusing on a smaller region of the spectrum (*i.e.* 495–520 nm), the forbidden Am^{III} $^5L_6 \leftarrow {}^7F_0$ transition was also observed as an absorption band in the excitation spectrum (Fig. 2), albeit as a slight feature centered at 508 nm, but only in the case of ligand **1**. This result is consistent with the energy levels of the respective ligand lowest T_1 excited states (Fig. 1): the intramolecular energy transfer from the chromophore triplet state can only occur with the lower-lying excited state of Am^{III} $^5D_1$ in the cases of ligands **2** and **3**, while excitation of **1** could result in the population of higher-energy levels such as $^5L_6$ (19 500 cm^{-1}) and up to $^5H_7$ (23 900 cm^{-1}).[29] The luminescence quantum yields of the three Am^{III} complex solutions were also noted to increase with higher chromophore T_1 excited state: the least efficient sensitization being observed with the Me-3,2-HOPO-based ligand **3** ($\phi = 1.3 \times 10^{-3}$%) and the most efficient with the 1,2-HOPO-containing ligand **1** ($\phi = 1.0 \times 10^{-2}$%). This trend is consistent with data obtained from the same Cm^{III} complexes, where all three types of chromophores can populate the emitting $^6D_{7/2}$ state, with respective luminescence quantum yields of 45%, 40%, and 16% for ligands **1**,[25] **2** (ESI Table S1†), and **3**,[25] respectively. Correspondingly, in the case of Eu^{III}, sensitization cannot occur with **3**, and a very weak emission (ϕ = 0.2%) was found with **2** (ESI Table S1†), since its triplet excited state energy lies only slightly higher than that of Me-3,2-HOPO and is too close to the $^5D_0$ state, resulting in inefficient energy transfer or back transfer to the triplet excited state. Similarly to what is reported with Sm^{III}, Dy^{III} or Nd^{III} species,[26,49] the luminescence quantum yields of the Am^{III} complexes are quite low due to the inherently low metal-centered luminescence of the Am^{III}, a consequence of the proximity between the highest ground state ($^7F_6$) and the emitting $^5D_1$ excited state (with an energy gap of only 4400 cm^{-1} based on calculations by Simoni *et al.*[50]). In addition, non-radiative decay from the $^5D_1$ state onto the non-emissive $^5D_0$ ground state in Am^{III} creates a rather efficient emission-quenching pathway in this actinide ion.

Time-resolved luminescence

Time-resolved analysis of the emitting complexes in H_2O revealed very fast luminescence decays in comparison with analogous Cm^{III},[25] Eu^{III}, and Tb^{III} species[28] (ESI Table S1†), with respective lifetimes of 42, 37, and 33 ns for **1**, **2**, and **3** (Table 1). As for the low quantum yields (*vide supra*), these short lifetimes are attributed to the narrow gap between the emitting $^5D_1$ state and the highest ground $^7F_6$ state. Such rapid decay patterns are commonly measured for Nd^{III} complexes and to a lesser extend for Sm^{III} and Dy^{III} compounds.[26,49] Kimura and coworkers have derived empirical methods to determine the number of inner sphere water molecules q in luminescent f-element complexes in aqueous solutions.[34,35] There is ample data for metal ions such as Cm^{III}, which increases the reliability of these methods and has led us to apply the derived equations to the HOPO ligand systems in previous reports.[25] Hence coordination numbers of 9, 10 and 10 were determined for the Cm^{III} complexes of **1** (q = 0.8), **2** (q = 4.2), and **3** (q = 2.5), respectively, and were confirmed using independent alternate calculations.[51] Likewise, a q = 0 value was determined and verified for the eight-coordinated $[Eu^{III}(\mathbf{1})]^-$ complex.[38,52] However, less data are available for Am^{III} compounds in general and, when applied to the present experimental lifetime values, this empirical method[35] provided unreasonably high q values of 4.7, 5.5, and 6.3 for **1**, **2**, and **3**, respectively. These results are incoherent with the similar sizes of the Cm^{3+} and Am^{3+} ions, with a slightly longer ionic radius for the latter, which would allow for an additional water molecule at most in comparison to Cm^{3+}. The short lifetimes observed here strongly suggest that energy transfer-back transfer with higher excited states occurs in Am(III) complexes, which may prevent the accurate use of empirical correlations. High uncertainties in these equations can also certainly arise from the presence of numerous N–H vibrations (like those found in the terminal amide functions of the HOPO or CAM units) that are known to quench luminescence lifetimes to some extent in visible emitters, such as Eu^{III}, and strongly in NIR emitters.[26,49] To address the applicability of the Kimura method to antenna-triggered luminescence, lifetimes were measured for $[Am^{III}(\mathbf{1})]^-$ after sequential additions of D_2O (Table 1 and ESI Fig. S2†), resulting in an only slightly slower luminescence decay of 73 ns in 50% D_2O, in contrast to a reported increase from 24 ns to 55 ns for the nona-aqua ion.[35] These experiments evidenced the little effect of D_2O when the metal center is chelated, suggesting less H–D exchange processes and fewer water molecules in the first coordination sphere than hypothesized by applying the Kimura equation, and another indication that N–H vibrations from the ligands have a substantial effect on the luminescence emission from the metal.

Solution thermodynamic characterization

As in our previous solution thermodynamic characterizations of f-element complexation by these high-affinity HOPO chelators,[25,28] the sensitized emission of the Am^{III} was used to determine the stability constants of the complex formed with the better sensitizer ligand **1**, through spectrofluorimetric indirect metal competition titrations at low micromolar concentrations (ESI Fig. S3†). Non-radioactive Eu^{III} was taken as a reference because of its electronic structure similar to that of Am^{III} and the remarkable luminescence properties of the corresponding complex, for which emission bands do not overlap with that of the Am^{III} complex. In these competition titrations, solutions containing an equimolar ratio of Am^{III} and **1** ([Am^{III}] = [**1**] = 3 μmol L^{-1}, [KCl] = 0.1 mol L^{-1}, [HEPES] = 0.1 mol L^{-1}, pH 7.4, 25 °C) were divided into separate aliquots and the competing Eu^{III} was added to reach concentrations varying from 0 to 15 μmol L^{-1}. The solutions were allowed to reach equilibrium (when no luminescence change was observed) and the emission spectra recorded (λ_{exc} = 325 nm). The intensity of the $[Am^{III}(\mathbf{1})]^-$ emission decreases

upon addition of Eu^{III} (ESI Fig. S3†), corresponding to the formation of the new complex. Fully reversed titrations were performed in the same manner, starting with solutions of Eu^{III} and **1** and using Am^{III} as the competing added metal. The data consisting of sets of emission spectra (λ_{em1} = 595–620 nm, λ_{em2} = 695–710 nm) with varying concentrations of competing metal were imported into the refinement program HypSpec[37] and analyzed by nonlinear least-squares refinements. The equilibration of **1** between both metals was calculated by including the proton association and Eu^{III} complex formation constants of the ligand, as well as the hydrolysis constants of both metals, as fixed parameters in the refinements, with the emission intensity resulting exclusively from the sensitization of the two metal ions by the ligand. Refinements yielded a complex formation constant $\log\beta_{110}$ = 20.4 ± 0.2 and corresponding $pM(Am^{III})$ value‡ of 21.3 ± 0.2. The stability of the Am^{III} complex of **1** falls well within the range observed in corresponding f-element complexes ($pM_{7.4}$ from 17.2 to 23.1 for the 4f series) and is equivalent to that of the Gd^{III} complex ($pM_{7.4}$ = 21.3).[28] As expected, it is also barely higher than that of the Eu^{III} complex ($pM_{7.4}$ = 21.1) but significantly lower than what is observed for Cm^{III} ($pM_{7.4}$ = 22.7).[25]

Density functional theory computational results

Density functional theory (DFT) calculations were employed to seek further insights into the metal–ligand interactions. Computational work was restricted to ligand **1**, based on the availability of complex coordinates from X-ray diffraction studies with $[Eu^{III}(\mathbf{1})]^{-0}$.[48] The structures of Eu^{III}, Am^{III}, and Cm^{III} complexes formed with ligand **1**, $[M^{III}(\mathbf{1})]^{-}$, were optimized, with resulting metal–oxygen distances listed in Table 2 and molecular orbital bonding analysis results illustrated in Fig. 4. Metal–oxygen distances were separated into two categories, depending on the chemical nature of the binding oxygen: the hydroxyl oxygens linked to nitrogen atoms display longer M–O distances by *ca.* 0.05 Å, as compared to the pyridinone oxygens linked to carbon atoms. The small differences in M–O distances among the three different metal species were also indicative of a strong ionic character in bonding: the four hydroxyl oxygens carry negative charges when deprotonated, displaying larger M–O bond distance variations than the pyridinone oxygens. However, based on the orbital analysis, overlap between the metal 5f orbitals and those of the ligand is higher with Cm^{III} than with Am^{III}, resulting in more covalent interactions. Owing to the large octadentate structure of the 1,2-HOPO ligand, many of the computed orbitals exhibited the same nature. We therefore used a simplified diagram to elucidate the frontier orbitals. In all three metal cases, the occupied frontier orbitals are the f-orbitals at the metal centre, while the π-bonding orbitals of the ligand lie below the f-orbitals. The bonding mixing between the ligand and metal d/f orbitals were omitted for clarity. The lowest unoccupied orbitals are dominated by the π*-antibonding orbitals of ligand **1**. Thus, excitation of ligand π-bonding orbitals is predicted to promote electrons to the π*-antibonding orbitals, which are higher in energy than the metal f-orbitals. The relaxation of these excited states will then sensitize the f-electrons and result in f → f transition decay, as observed experimentally.

Table 2 Metal–oxygen bond distances from predicted geometric structures of Eu^{III}, Am^{III} and Cm^{III} complexes formed with ligand **1**[a]

Bond length (Å)	Eu^{III}	Am^{III}	Cm^{III}
M–O(–N)	2.478	2.487	2.483
M–O(–C)	2.430	2.437	2.437

[a] Elements in parentheses are those connected to the oxygen atom.

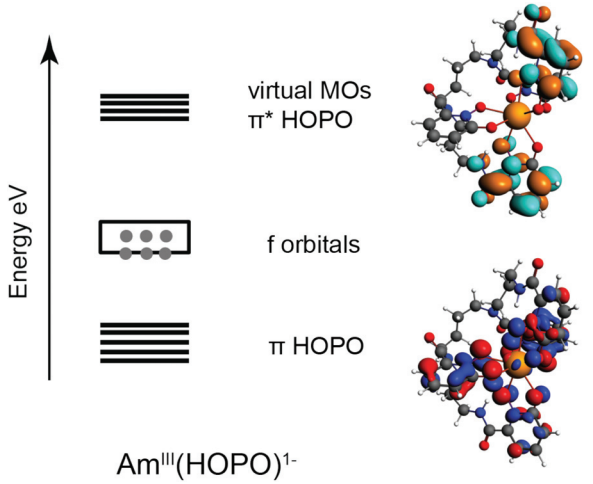

Fig. 4 Molecular orbital diagram of $[Am^{III}(\mathbf{1})]^{-}$, with "HOPO" designating ligand **1**. The respective natures of frontier orbitals are listed by their main contributors. The isosurface value for the MO orbitals is 0.03.

Nephelauxetic effect and bonding strength

The bathochromic shift of the emission maxima observed during complexation of Ln^{III} and An^{III} cations is induced by the relative decrease in inter-electronic repulsion, and is correlated with the nephelauxetic effect. While the shifts observed with 4f species are typically small (0–3 nm range, corresponding to an energy shift of less than 65 cm^{-1}),[53] shifts as large as 50 nm (corresponding to ~1100 cm^{-1}) have been noted in 5f systems.[54] When choosing the transition from the lowest Stark level of the excited state $^5D_1$ to the ground level of the accepting state $^7F_1$, shifts of about 9, 4, and 6 nm were observed in the complexation of Am^{III} by **1**, **2**, and **3**, respectively, with 689 nm as the reference for the free ion in solution.[13] These shifts are of the order of 1% and are therefore remarkably less pronounced than those observed with the corresponding Cm^{III} complexes (*ca.* 2.5%).[25] Most theoretical studies of the nephelauxetic effect have investigated series of ligands for individual cations,[53,54] but have seldom provided comparisons among analogous complexes through the 4f and 5f series. A recent study established that the nephelauxetic parameter increased regularly with increasing Z in series of allyl acetoacetate lanthanide complexes.[55] This trend is

consistent with the increasing effects observed here when replacing Am^{III} by Cm^{III}. The experimental formation constants of the complexes formed with ligand **1** increased in the 4f series with decreasing metal ionic radius and also increased from Am^{III} to Cm^{III}. This could simply be explained by ionic metal–ligand bonding. However, the observed nephelauxetic shift of the emitting f–f transitions in the 5f complexes could also indicate partial covalency in the metal–ligand bonds, which is corroborated by the increased metal–ligand orbital overlap observed in the computed structures when substituting Am^{III} for Cm^{III}. In addition, the significantly shorter M–O bond distances observed in the calculated $[Eu^{III}(1)]^-$ structure contrast with a slightly lower complex stability, as compared to the Am^{III} species, which implies increased covalency in the 5f complexes. Comparisons among ligands for a same metal ion are slightly more intricate, as the shift may be due to a combination of factors such as the coordination number or the basicity of the different ligands.

Conclusions

We report the first characterization of Am^{III} luminescence sensitization by three antenna ligands, 3,4,3-LI(1,2-HOPO), Enterobactin, and 5-LIO(Me-3,2-HOPO). Those ligands were initially probed based on their ease of production and availability due to on-going pharmaceutical development studies, but it had become apparent that their respective triplet excited state energies are adequately situated at higher levels than accepting Am^{III} levels. The photophysical properties of the resulting Am^{III} complexes have revealed intramolecular energy transfer processes with features specific to the electronic structure of the Am^{3+} ion and drastically different from those of corresponding Eu^{III} and Cm^{III} complexes. As further evidenced through the determination of solution thermodynamic parameters for the complexation of Am^{III}, the use of steady-state luminescence spectroscopy may become an important tool for actinide speciation in complex environments. Future studies will focus on fine-tuning ligand structures to regulate these luminescence sensitization processes with actinide ions and establish direct correlations between stability and spectroscopic properties of the complexes with coordination numbers and electronic structures of both the ligand and the chelated element.

Acknowledgements

Enterobactin was a generous gift from Prof. Kenneth N. Raymond (University of California, Berkeley). This material is based upon work supported by the U.S. Department of Energy, Office of Science Early Career Research Program and Office of Science, Office of Basic Energy Sciences, Chemical Sciences, Geosciences, and Biosciences Division at the Lawrence Berkeley National Laboratory under Contract DE-AC02-05CH11231 (RJA). RJA is the recipient of a U.S. Department of Energy, Office of Science Early Career Award. Computational work was supported by the U.S. Department of Energy, Office of Science, Basic Energy Sciences, Chemical Sciences, Biosciences, and Geosciences Division (CSGB), Heavy Element Chemistry Program at Los Alamos National Laboratory under contract no. DE-AC52-06NA25396 (operated by Los Alamos National Security, LLC, for the National Nuclear Security Administration of the U.S. Department of Energy) (PY). The DFT calculations were performed using the Molecular Science Computing Facilities in the William R. Wiley Environmental Molecular Sciences Laboratory, a U.S. Department of Energy Office of Science User Facility sponsored by the Office of Biological and Environmental Research and located at Pacific Northwest National Laboratory.

Notes and references

1 L. W. Davis, *J. Econ. Perspect.*, 2012, **26**, 49–66.
2 IAEA, *Nuclear Technology Review*, 2013.
3 P. A. Baisden and C. E. Atkins-Duffin, in *Handbook of Nuclear Chemistry*, ed. A. Vertes, S. Nagy, Z. Klenesar, R. G. Lovas and F. Rosch, Springer, Dordrecht, Heidelberg, London, New York, 2nd edn, 2011, vol. 5, ch. 61.
4 B. Barre, *J. Alloys Compd.*, 1998, **271–273**, 1–5.
5 T. L. Griffiths, L. R. Martin, P. R. Zalupski, J. Rawcliffe, M. J. Sarsfield, N. D. M. Evans and C. A. Sharrad, *Inorg. Chem.*, 2013, **52**, 3728–3737.
6 T. Kooyman and L. Buiron, *EPJ Nuclear Sci. Technol.*, 2015, **15**, 1–8.
7 M. J. Polinski, D. J. Grant, S. A. Wang, E. V. Alekseev, J. N. Cross, E. M. Villa, W. Depmeier, L. Gagliardi and T. E. Albrecht-Schmitt, *J. Am. Chem. Soc.*, 2012, **134**, 10682–10692.
8 K. L. Nash, C. Madic, J. N. Mathur and J. Lacquement, in *The Chemistry of the Actinide and Transactinide Elements*, ed. L. R. Morss, N. M. Edelstein and J. Fuger, Springer, Dordrecht, The Netherlands, 2006, vol. 4, pp. 2622–2798.
9 J. C. Braley, J. C. Carter, S. I. Sinkov, K. L. Nash and G. J. Lumetta, *J. Coord. Chem.*, 2012, **65**, 2862–2876.
10 J. C. Braley, T. S. Grimes and K. L. Nash, *Ind. Eng. Chem. Res.*, 2012, **51**, 629–638.
11 J. D. Burns, T. C. Shehee, A. Clearfield and D. T. Hobbs, *Anal. Chem.*, 2012, **84**, 6930–6932.
12 *Luminescence of Lanthanide Ions in Coordination Compounds and Nanomaterials*, ed. A. de Bettencourt-Dias, John Wiley and Sons, Hoboken, 2014.
13 J. V. Beitz, *J. Alloys Compd.*, 1994, **207**, 41–50.
14 L. S. Natrajan, *Coord. Chem. Rev.*, 2012, **256**, 1583–1603.
15 J. R. Peterson, *J. Alloys Compd.*, 1995, **225**, 11–14.
16 Z. Assefa, T. Yaita, R. G. Haire and S. Tachimori, *Inorg. Chem.*, 2003, **42**, 7375–7377.
17 Y. A. Barbanel, G. P. Chudnovskaya, Y. I. Gavrich, R. B. Dushin, V. V. Kolin and V. P. Kotlin, *J. Radioanal. Nucl. Chem.*, 1990, **143**, 113–123.
18 A. Barkleit, G. Geipel, M. Acker, S. Taut and G. Bernhard, *Spectrochim. Acta, Part A*, 2011, **78**, 549–552.

19 I. Billard and G. Geipel, in *Standardization and Quality Assurance in Fluorescence Measurements I*, ed. U. Resch-Genger, Springer, Berlin Heidelberg, 2008, vol. 5, ch. 50, pp. 465–492.
20 G. Geipel, *Coord. Chem. Rev.*, 2006, **250**, 844–854.
21 B. Raditzky, S. Sachs, K. Schmeide, A. Barkleit, G. Geipel and G. Bernhard, *Polyhedron*, 2013, **65**, 244–251.
22 T. Stumpf, M. M. Fernandes, C. Walther, K. Dardenne and T. Fanghaenel, *J. Colloid Interface Sci.*, 2006, **302**, 240–245.
23 B. E. Allred, P. B. Rupert, S. S. Gauny, D. D. An, C. Y. Ralston, M. Sturzbecher-Hoehne, R. K. Strong and R. J. Abergel, *Proc. Natl. Acad. Sci. U. S. A.*, 2015, **112**, 10342–10347.
24 M. Sturzbecher-Hoehne, C. Goujon, G. J. P. Deblonde, A. B. Mason and R. J. Abergel, *J. Am. Chem. Soc.*, 2013, **135**, 2676–2683.
25 M. Sturzbecher-Hoehne, B. Kullgren, E. E. Jarvis, D. D. An and R. J. Abergel, *Chem. – Eur. J.*, 2014, **20**, 9962–9968.
26 A. D'Aleo, F. Pointillart, L. Ouahab, C. Andraud and O. Maury, *Coord. Chem. Rev.*, 2012, **256**, 1604–1620.
27 D. I. Bunin, P. Y. Chang, R. S. Doppalapudi, E. S. Riccio, D. An, E. E. Jarvis, B. Kullgren and R. J. Abergel, *Radiat. Res.*, 2013, **179**, 171–182.
28 M. Sturzbecher-Hoehne, L. Clara Ng Pak, A. D'Aleo, B. Kullgren, A.-L. Prigent, D. K. Shuh, K. N. Raymond and R. J. Abergel, *Dalton Trans.*, 2011, **40**, 8340–8346.
29 W. T. Carnall, *J. Chem. Phys.*, 1992, **96**, 8713–8726.
30 R. D. Shannon, *Acta Crystallogr., Sect. A: Cryst. Phys., Diffr., Theor. Gen. Cryst.*, 1976, **32**, 751–767.
31 K. Binnemans, *Coord. Chem. Rev.*, 2015, **295**, 1–45.
32 A. B. Yusov, *J. Radioanal. Nucl. Chem.*, 1990, **143**, 287–294.
33 P. Y. Chang, D. I. Bunin, J. Gow, R. Swezey, W. Shinn, D. K. Shuh and R. J. Abergel, *J. Chromatogr. Sep. Tech.*, 2012, S4.
34 T. Kimura and G. R. Choppin, *J. Alloys Compd.*, 1994, **213–214**, 313–317.
35 T. Kimura and Y. Kato, *J. Alloys Compd.*, 1998, **271–273**, 867–871.
36 P. Gans, A. Sabatini and A. Vacca, *Talanta*, 1996, **43**, 1739–1753.
37 P. Gans, A. Sabatini and A. Vacca, *HypSpec*, Leeds, U.K. Florence, Italy, 2008.
38 R. J. Abergel, A. D'Aleo, C. N. P. Leung, D. K. Shuh and K. N. Raymond, *Inorg. Chem.*, 2009, **48**, 10868–10870.
39 A. E. Martell, R. M. Smith and R. J. Motekaitis, *NIST Standard Reference Database 46*.
40 L. Alderighi, P. Gans, A. Ienco, D. Peters, A. Sabatini and A. Vacca, *Coord. Chem. Rev.*, 1999, **184**, 311–318.
41 L. Alderighi, P. Gans, A. Ienco, D. Peters, A. Sabatini and A. Vacca, *HYSS*, Leeds, U.K. Florence, Italy, 2009.
42 J. P. Perdew, K. Burke and M. Ernzerhof, *Phys. Rev. Lett.*, 1996, **77**, 3865–3868.
43 *ADF2014*, SCM, Theoretical Chemistry, Vrije Universiteit, Amsterdam, The Netherlands.
44 C. Fonseca Guerra, J. G. Snijders, G. te Velde and E. J. Baerends, *Theor. Chem. Acc.*, 1998, **99**, 391–403.
45 G. te Velde, F. M. Bickelhaupt, E. J. Baerends, C. Fonseca Guerra, S. J. A. van Gisbergen, J. G. Snijders and T. Ziegler, *J. Comput. Chem.*, 2001, **22**, 931–967.
46 E. van Lenthe, E. J. Baerends and J. G. Snijders, *J. Chem. Phys.*, 1993, **99**, 4597–4610.
47 E. van Lenthe and E. J. Baerends, *J. Comput. Chem.*, 2003, **24**, 1142–1156.
48 L. J. Daumann, D. S. Tatum, B. E. R. Snyder, C. Ni, G.-L. Law, E. Solomon and K. N. Raymond, *J. Am. Chem. Soc.*, 2015, **137**, 2816–2819.
49 A. D'Aleo, A. Bourdolle, S. Brustlein, T. Fauquier, A. Grichine, A. Duperray, P. L. Baldeck, C. Andraud, S. Brasselet and O. Maury, *Angew. Chem., Int. Ed.*, 2012, **51**, 6622–6625.
50 R. Cavellec, S. Hubert and E. Simoni, *J. Solid State Chem.*, 1997, **129**, 189–195.
51 G. Tian, N. M. Edelstein and L. Rao, *J. Phys. Chem. A*, 2011, **115**, 1933–1938.
52 R. M. Supkowski and W. D. Horrocks, *Inorg. Chim. Acta*, 2002, **340**, 44–48.
53 P. Dorenbos, *J. Lumin.*, 2013, **136**, 122–129.
54 Y. A. Barbanel, *Radiochim. Acta*, 1997, **78**, 91–95.
55 A. M. Mishchenko, E. K. Trunova, A. S. Berezhnytskaya and A. A. Rogovtsov, *J. Appl. Spectrosc.*, 2015, **81**, 905–911.